Volume 9, Issue 6, 2019, 4617 - 4623 ISSN 2069-5837

Biointerface Research in Applied Chemistry

www.BiointerfaceResearch.com

https://doi.org/10.33263/BRIAC96.617623

Original Research Article Open Access Journal

Received: 30.09.2019 / Revised: 12.11.2019 / Accepted: 13.11.2019 / Published on-line: 20.11.2019

Synthesis and characterization of nontoxic silver nano-particles with preferential bactericidal activity

Ghareib W. Ali [1,*], Sh. I. Abd El-Moez [2], Wafa. I. Abdel-Fattah [1]

[1] Refractories, Ceramics, Building materials Dept.: Biomaterials Group, National Research Centre (NRC), Tahrir Street, Dokki, Cairo, 12311, Egypt

[2] Microbiology& immunology Dept., Vet. Division, National Research Centre (NRC), Tahrir Street, Dokki, Cairo, 12311, Egypt

*corresponding author e-mail address: ***wafaaghareib@gmail.com*** | Scopus ID 56644204600

ABSTRACT

The massive prophylactically or remedially application of antibiotics without proper medical indications lead to severe problems of bacterial resistance. Nanoparticles (NPs) are increasingly applied to target bacterial infections as an antibiotic alternative. Green synthesis of silver nanoparticles (AgNPs), with controlled morphology, within cinnamon extract using microwave irradiation was carried out. The influence of the pH on the synthesized AgNPs was assessed. Physicochemical characterizations were followed through UV, FTIR, FESEM, HRTEM, XPS and XRD analyses. Bactericidal activity and *in-vitro* cytotoxicity of the achieved AgNPs were investigated. Results proved the successful synthesis of spherical AgNPs with an average size of 15 nm. The AgNPs safety was verified through cytotoxicity test against skin fibroblast normal cells. The obtained AgNPs exhibited promising bactericidal activities against the screening of several Gram+ve and Gram-ve bacteria. Therefore, it can be successfully applied in the biomedical fields for hard and soft tissue remedies.

Keywords: *Silver nanoparticles; Cinnamon extract, microwave; Cytotoxicity, antibacterial screening.*

1. INTRODUCTION

Research for novel, efficient bactericidal materials is significantly increased for combatting drug resistance. Nanoparticles are synthesized following several approaches as chemical [1], bio-reduction [2], electrochemical reduction [3], photochemical reduction [4], and heat evaporation [5]. However, biological routes for the NPs synthesis using enzymes [6], microorganisms [7], and plant extracts [8] present facile, cost-effective and eco-friendly routes since no toxic reducing or stabilizing agents are involved in the synthesis process. Moreover, it can be scaled up easily for large-scale production. The greenly plant-based synthesized silver nanoparticles represent a promising source for several novel bactericidal agents because of their multi-targeting action mechanism. In particular, nano-silver has been verified to have a high medicinal value attributed to its unique antibacterial [9], antifungal [10], antiviral [11], antiprotozoal [12], anticatalytic [13] and anti-arthropodal characteristics [14].

Plants can assist the reduction of silver ions through its variable metabolites. Additionally, it is readily available at low cost [15]. Recently, several manuscripts were reported for the synthesis of gold (Au), silver (Ag), and palladium (Pd) nanoparticles using plant extracts as Geranium leaf [16], Aloe vera [17], Lemongrass [18], and BlackBerry [19].

In this context, cinnamon plant extract has a long history in biomedical applications [20]. It can be directly applied as a reducing and stabilizing agent in synthesize of biocompatible AgNPs from silver salt precursors. Cinnamon phytochemical constituents include about 1–4% of essential oil, polyphenols (5–10%), carbohydrates (80–90%), and other ingredients including gum, mucilage, resin and calcium mono terpenes oxalate [21-23]. The essential oil has been primarily characterized as aldehydes (60–80%), including trans-cinnamaldehyde. Cinnamaldehyde in combination with other related organic alcohols constitutes the primary phytochemicals that give the cinnamon its aroma characteristics [24-26]. The cinnamon phytoconstituents contain functional groups (aldehyde and hydroxyl units within the molecular framework) and carbohydrates (starch and polysaccharides). These functional groups provide a synergistic chemical reduction ability for the Ag precursor to synthesis and stabilize AgNPs in a single green process.

Recently, microwave-assisted synthesis is widely applied to produce several nanoparticles [27]. In comparison to convenient hydrothermal methods, the microwave has the advantages of being quick, simple and short time reaction resulting in the controllable morphology of the developed nano-particles. In the present research, green synthesis of AgNPs within the aqueous extract of cinnamon bark was successfully achieved thereby, leading to nonpolluting, eco-friendly nanoparticles. The cytotoxicity against normal cell line was investigated. Further, screening the activities of the achieved green silver nanoparticles was compared to the mother cinnamon bark extract against several G+ve and G-ve bacterial strains.

2. MATERIALS AND METHODS

2.1. Extract preparation. Cinnamon bark extract was achieved via heat treatment. Ten grams of cinnamon powder within 100 ml of deionized water was heated at 70 °C for one hour. The filtered extracts were stored at 4°C for further experiments.

2.2. Synthesis of the biogenic Ag nanoparticles. Silver nitrate ($AgNO_3$, MWt. 169.87 g/mole, Aldrich) was used as a silver precursor. Fifty ml of extract were mixed with silver nitrate aqueous solution with four concentrations being 0.1, 0.5, 1 and 1.5

mg/ml. The obtained mixtures were subjected to microwave heating for several periods. A pulsed mode of on 5 s, off 5 s was applied to prevent intense boiling and particle aggregation. The achieved nanoparticles were stored at 4°C for further characterization and bio-applications.

2.3. Characterization.

2.3.1. Physico-chemical characterization. UV–Vis absorption spectra of the achieved AgNPs were obtained using Junway 6100 spectrophotometer within the range of 200–1000 nm semi-quantitatively.

X-ray powder diffraction (XRD) analyses were achieved using Cu Kα radiation (l=1.5418 Å) at a scanning speed of 0.3 S (Philips X'pert Pro X-ray powder diffractometer). The applied voltage and current were 40 kV and 40 mA respectively.

Fourier Transform Infrared (FTIR) spectra were recorded using Vertex 70 Bruker optics, Germany spectrometer. The spectra were collected using a spectral resolution of 4.0 cm^{-1} and 64 scans were accumulated to get a reasonable signal to noise ratio. The determination of the ζ-potential of the developed AgNPs was carried out using a Malvern Nano ZS instrument.

Field Emission Scanning Electron Microscopy (FESEM) was performed using a Quanta FEG 250-type microscope equipped with an energy dispersive X-ray attachment (EDAX/Genesis device). The morphology of the developed nanoparticles was investigated by HRTEM (JEM 2010 instrument) at an accelerating voltage of 200 kV equipped with selected area electron diffraction facility (SAED). A drop of the nanoparticles solution was placed onto a carbon film supported on a copper grid and left to dry at room temperature. The surface species of the synthesized nanoparticles were depicted by X-ray Photoelectron Spectroscopy (XPS) on an AXIS ULTRA DLD spectrometer with AlK-α radiation (hν =1486.71 eV) with an energy resolution of 0.48 eV. XPS analyses were conducted at 150Watt (W) and a pass energy of 16 electron volt (eV). The Ag concentrations within the prepared synthesis solutions pre- post-reduction were measured on Agilent 5100 Inductively Coupled Plasma Optical Emission Spectrometer (ICP-OES) with Synchronous Vertical Dual View (SVDV).

2.3.2. Cytotoxic activity. *In-vitro* cytotoxicity was investigated against normal skin fibroblast normal cells (BJ1) cell line by MTT assay 3- [4, 5-dimethylthiazol-2-yl]-3, 5-diphenyltetrazolium bromide dye. Cells were inserted in a 96-well plate at a density of 1×10^4 cells per well. The media were inoculated with 1% antibiotic–anti-mycotic mixture which is composed of 10,000 U mL^{-1} potassium penicillin, 10,000 µg/mL streptomycin sulfate, 25 µg/mL amphotericin B and 1% L-glutamine (Bio west, USA). Further, the media were incubated at 37°C in a humidified atmosphere with 5% CO_2. Post cells attachment, the media were replaced by the nanoparticles for 72 hours. The cells were incubated with the MTT solution (5.0 mg/mL) at 37°C for four hours. The purple formazan crystals developed were dissolved in 100 µL dimethyl sulfoxide (DMSO) and recorded (ELISA reader). The cell viability % was calculated by the following equation (1):

$$\textbf{Viability}\ \% = \frac{\mathbf{OD_{test} - OD_{blank}}}{\mathbf{OD_{control} - OD_{blank}}} \boldsymbol{x100}$$

OD_{test}: Mean value of sample absorbance measured at 570 nm.

OD_{blank}: Mean value of blank absorbance measured at 570 nm.

$OD_{control}$: Negative Control.

2.3.3. Bactericidal activity and screening. Evaluation of the antimicrobial activities was carried out using the agar well diffusion method as a qualitative technique [28]. The bactericidal activities of the synthesized AgNPs within the cinnamon extract were tested against Gram-negative bacteria (*Salmonella typhimurium ATCC14028, Shigella flexneri ATCC12022, E. coli O157 ATCC700728, E. coli ATCC25922 and Vibrio parahaemolyticus ATCC10885*), Gram-positive bacteria (*Cl. perfringens ATCC13124, Staphylococcus aureus ATCC6538, Bacillus cereus ATCC10876, Listeria innocuous ATCC33090, Enterococcus fecalis ATCC11700 and Listeria monocytogenes ATCC35152*). Moreover, AgNPs were tested against Candida albicans ATCC2091 Mycotic strain. As a control, the positive Antibiotic Ciprofloxacin (CIP5) (5µg/ml) was used as standard antibacterial while Antimycotic (AMB20) was used as a standard antifungal. Moreover, dimethyl sulphoxide (DMSO) was used as a negative control. The Muller Hinton agar plates were inoculated with the bacterial and fungal strains prepared in a concentration equivalent to 0.5 McFarland for bacterial strains and 2×10^5 and streaked onto the agar plates using sterile swabs, under sterile conditions, 80 µl of the tested samples were placed into the wells. Plates were incubated at 37˚C/24 hour aerobically. Conversely, Cl. perfringens plates were incubated at 37˚C/24 hour anaerobically for bacterial growth. On the other hand, *C. albicans* plates were incubated at 28˚C/48-72 hour for fungal growth. Inhibition zones were measured in mm. The experiments were carried out in triplicates. The Mean ± SE of the inhibition zones were calculated.

3. RESULTS

3.1. Physicochemical characterization.

The Ag precursor concentrations effect was followed to optimize the functional concentration. Several concentrations ranging from 0.001-0.015 mg/ml were examined. The increase in the absorbance values upon increasing Ag concentration demonstrates the higher production of Ag nanoparticles. The achieved optimum SPR is corresponding to the Ag concentration of 0.001-0.015 mg/ml (Fig. 1(a)).

AgNPs solution was synthesized within several pH values covering a range of 3-11. Their corresponding UV surface plasmon resonance (SPR) is represented in figure 1. The intensity of the color is affected by changing the pH of the developed AgNPs due to excitation of surface plasmon vibrations in the metal nanoparticles. The sharp peak at 429 nm is denoted for the SPR of the AgNPs [29]. The SPR at physiological pH=7 possessed the optimum AgNPs size distribution. Therefore, it was selected for further bactericidal applications. At lower pH, the aggregation of AgNPs leads to more massive nanoparticles. Conversely, at higher pH, a large number of the functional groups were available for silver binding and subsequently resulted in a higher number of nanoparticles with smaller diameters. Moreover, by elevating the pH, the shape of the achieved nanoparticles was more spherical rather than ellipsoidal. This result confirms the crucial role played by pH in controlling the shape and size of the synthesized Ag nanoparticles.

SPR spectra of the synthesized nanoparticles at several pH conditions are presented in figure 1 (b). At pH 3, a straight absorption spectrum was recorded. Weak SPR peaks were formed under acidic conditions thus terming it as unsuitable for promoting the biosynthesis of silver nanoparticles. Conversely, neutral and alkaline conditions demonstrate sharp SPR peaks indicating the appropriate values for AgNPs biosynthesis. The higher SPR peak intensities corresponding to the alkaline medium possessed an increased number of smaller silver nanoparticles. The peak signifies uniformly shaped nanoparticles [30].

Hence, the alkaline condition is favorable as the hydroxides get deposited on the silver nanoparticle due to alkalinity. Moreover, at the alkaline pH, the capping agents efficiently reduce the particles and further capped them at specific facets. Consequently, it allows spherical nanoparticles growth due to vulnerable Ag atomic deposition on all the facets developing; therefore, the thermodynamically favorable spherical NPs [31]. Conversely, the high proton concentration at acidic pH possessed a positive charge for all the functional groups responsible for NPs biosynthesis. Consequently, the reducing power of these functional groups is decreased [32].

The band gap was calculated applying Tacu's relationship:

$$\alpha = \alpha_0 \frac{\left(h\nu - E_g\right)^n}{h\nu}$$

Where α is the absorption coefficient, hυ is the photon energy, α_0 is constant, h is Blank's constant and E_g is the optical band gap; n depends on the electronic transition type and can be ranged from 1/2 to 3. The AgNPs energy gaps were calculated by extrapolating the linear portion of the plots of $\alpha h\nu^2$ versus hν to the energy axis. Figure 1 (c, d) depicts an indirect electronic transition for the optimum AgNPs. The Eg values were 2.1, 1.82, 1.5, 1.48, 1.38 eV for AgNPs at pH=3, 5, 7 and 9 respectively. Figure 1 (d) illustrates the inversely proportional relationship between the pH and the band gap energy values.

FTIR spectra of the biogenic AgNPs provided evidence for the cinnamon specific functional groups ability to reduce Ag ions (Fig. 2 (a)). The cinnamon extract and cinnamon mediated AgNPs spectra displayed a specific band corresponding to aromatic CH bonds at 3473 cm^{-1}. The band at 1635 cm^{-1} is attributed to C=C [33]. The absorption peak at 3432 cm^{-1} is assigned to N–H stretching vibration [34], whereas the band at 2925 cm^{-1} is associated with the C–H stretching vibration-asymmetric [35, 36]. The peak at 1385 cm^{-1} is corresponding to C–H symmetric deformation vibration [37] while the one at 1033 cm^{-1} is assigned to C–O stretching [38]. The slight shift and reduced intensity of the cinnamon mediated AgNPs spectrum are attributed to the involvement of the cinnamon functional groups in the AgNPs bio-reduction process.

The present successful reduction of Ag precursor within cinnamon extract through microwave is attributed to the triggered reduction potential of its terpenoids, including linalool, eugenol, methyl chavicol, cinnamaldehyde, ethyl cinnamate and -caryophyllene, which contribute to its distinct aroma [39]. Terpenoids are believed to play an essential role in AgNPs biosynthesis through the reduction of Ag ions. Also, several proteins within the cinnamon bark are reported to bind with the nanoparticles either through free amine groups or the proteins cysteine's residues. A similar mechanism should have operated in the present conditions where the proteins extracted from the cinnamon bark capped the Ag nanoparticles, thereby stabilized them.

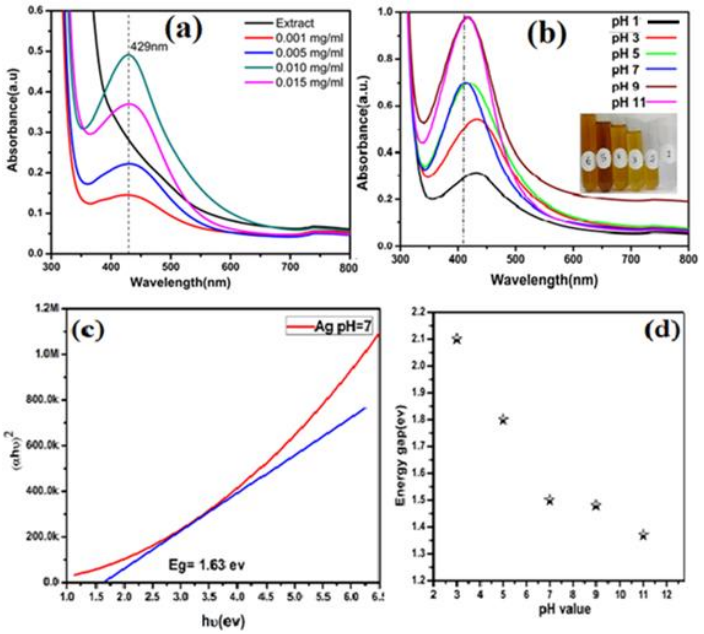

Figure 1. UV-Vis spectra for the biogenic AgNPs (a) Effect of silver ions concentrations and (b) Effect of media pH on the development of AgNPs. (c) Band gap energy of AgNPs at pH=7 (d) relation between pH values and band gap energy.

The AgNPs stability and mucoadhesion were characterized by measuring its zeta potential. Charges of the selected AgNPs configurations were negative. Higher electrostatic stability of the AgNPs is proved at higher pH values, as it is directly proportional to zeta potential value.

Figure (2 (b)) shows the effect of pH values on the zeta potential of the achieved AgNPs. The absolute value of the negative zeta potential increased upon increasing pH. This direct proportionality is explained by the instability of the nanoparticles at acidic pH. The zeta potential results are coinciding with the UV-Vis spectra.

The crystalline nature of the developed AgNPs was investigated by X-ray diffraction technique. XRD patterns are shown in figure (2 (c, d)). The figure shows the major AgNPs (111) plane within the cinnamon extract. The silver nanoparticles spectrum exhibited clear peaks of cubic phase (JCPDS No. 03-0921) at 2θ =38.7 (1 1 1), 44.5 (2 0 0), 64.5 (2 2 0) coinciding with the TEM results [40-41].

The selected AgNPs solutions were analyzed using ICP. The conversion% of the silver ions into silver nanoparticles was calculated using the following equation (2).

$$X\,\% = \frac{C_0 - C_F}{C_0} x100$$

Where X denotes the conversion of silver ions to silver nanoparticles; C_0 is the initial concentration of silver ions in the solution; and C_f is their final concentrations in the solution [30]. The success of the presently applied green synthesis route was assured since the calculated conversion ratio was 96.16%.

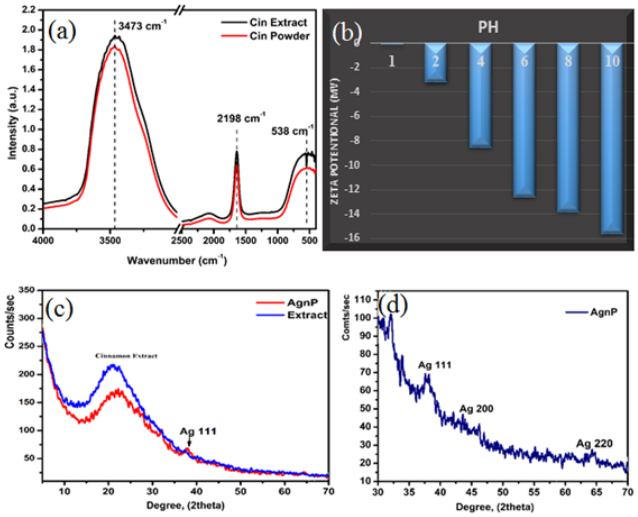

Figure 2. (a) FTIR spectrum depicts the functional groups of the cinnamon extract and AgNPs (b) Zeta potential of the developed AgNPs at several pH values. XRD patterns of (C) cinnamon extract and AgNPs (d) excluded AgNPs pattern.

Figure 3 shows the TEM images of the developed Ag nanoparticles synthesized within cinnamon extract via microwave treatment. Most of the nanoparticles were roughly spherical having smooth edges with an average size of 12 nm. Some nanoparticles proved anisotropic nanostructures with irregular contours. The selected area electron diffraction (SAED) rings showed a face-centered cubic (FCC) structure indicating the polycrystalline nature of the silver nanoparticles. The bright and regular crystal Debye Scherrer rings are proving the high crystalline nature of the achieved silver nanoparticles. The lattice diffraction rings are corresponding to the Ag (111), (200), (220) and (311) planes.

FESEM images of the achieved AgNPs are shown in figure 4. Bright crystalline AgNPs uniformly distributed within the cinnamon extract confirming, therefore, its successful achievement. The bright features of the scanned silver nanoparticles proved its crystallinity.

XPS Survey narrow scan spectra of the developed silver nanoparticles are represented in figure 5. The main peaks of Ag3d binding energies have arisen at 377 eV. The cinnamon C-C binding energies are depicted at 285 eV while the O1s recorded at 530 eV.

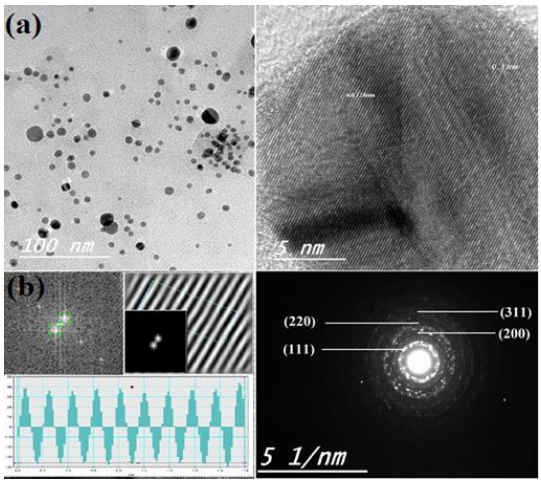

Figure 3. (a) HRTEM image of the developed AgNPs, (b) SAED pattern with crystalline features.

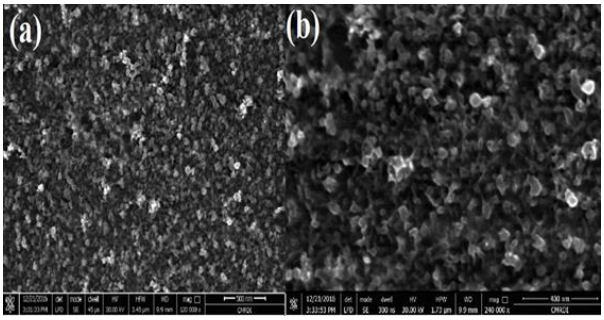

Figure 4. FESEM images of the synthesized AgNPs (a) lower magnification (b) Higher magnification showing the bright crystalline silver nanoparticles.

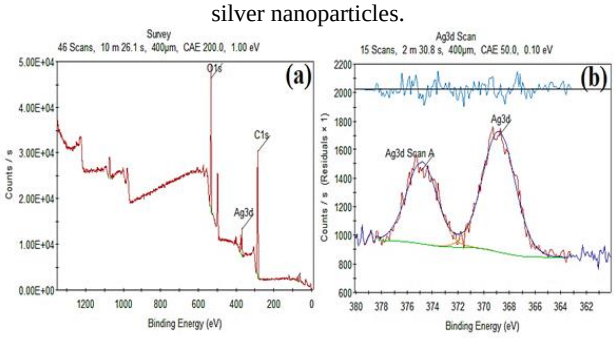

Figure 5. a) XPS complete survey of the synthesized AgNPs b) corresponding deconvoluted XPS narrow scan spectra of AgNPs.

3.2. Biological implications.

3.2.1. ***In-vitro cytotoxicity.*** *In-vitro* cytotoxicity test is a vital requirement for biomaterials assessment to satisfy its suitability for biomedical applications. Moreover, it recognizes its limitations [42]. The viability percentage of the achieved AgNPs was evaluated against skin fibroblast normal cells (BJ1). The viability % was calculated to be 99. The high viability % was proving, therefore, the safety features of the synthesized silver nanoparticles for its intended biomedical applications.

3.2.2. ***Bactericidal activity.*** The bactericidal activities of the achieved AgNPs were tested against Gram-positive and Gram-negative bacteria. The anti-fungal activity was investigated against *Candida albicans* ATCC2091 Mycotic strain (Fig. 6).

Seldom cinnamon extract exhibited promising bactericidal activity against *S. aureus* with an inhibition zone of 16.67±0.67 mm. Additionally, it possessed an enhanced hindrance against *L. innocus*, *E. coli*, *S. flexeneri*. Conversely, it has some limited hindrance activities against *S. typhimurium*, *L. moncytogenes* and *V. parahaemolyticus*.

Interestingly, the silver nanoparticles possessed a hindrance activity against the tested reference strains. The eclecticism bactericidal activities were demonstrated against *E. coli* O157 with an inhibition zone of 22.00±1.5mm, followed by *V. parahaemolytica* and *L. monocytogenes* with an inhibition zone of 20.67±0.67mm. Silver nanoparticles within cinnamon extract showed promising activities against *L. monocytogenes* and Vibrio parahaemolyticus with a zone of inhibition 22.00±1.15 and 21.00±0.58mm respectively. Results were compared with the control negative (DMSO) showing negative hindrance activities. The control positive reference drug, antibiotic CIP (5µg) and Amphotericin B (20µg/ disc) exhibited the best hindrance activities against tested reference cultures.

Although the exact mechanism for the growth inhibition by Ag nanoparticles has not yet been elucidated, many possible mechanisms have been proposed. Generally, Ag ions from

nanoparticles are believed to become attached to the negatively charged bacterial cell wall and rupture it, leading to protein denaturation and finally cell death [43].

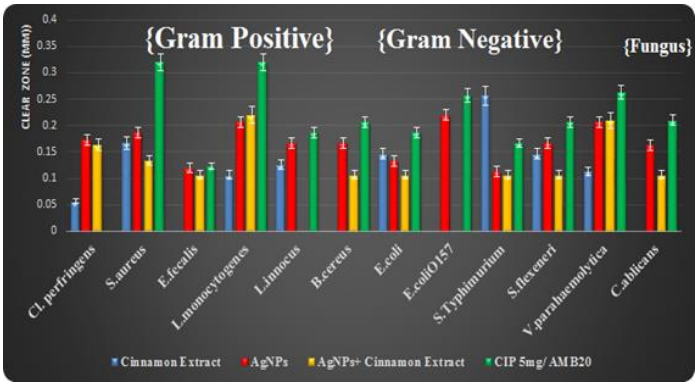

Figure 6. Bactericidal activity of the developed AgNPs compared with cinnamon extract against twelve bacterial strains.

The attachment of either Ag ions or nanoparticles to the cell wall causes accumulation of envelope protein precursors resulting in dissipation of the proton motive force. Ag nanoparticles also exhibited destabilization of the outer membrane and rupture of the plasma membrane, thereby causing depletion of intracellular adenosine triphosphate (ATP) [44]. Another proposed mechanism involves the association of silver with oxygen and its reaction with sulfhydryl (–S–H) groups on the cell wall to form R–S–S–R bonds, thereby blocking respiration and causing cell death [45]. Similar modes of action have been reported for Ag nanoparticles and Ag ions, although Cho et al. reported that the nanoparticles were effective at significantly lower concentrations [46]. In contrast, Morones et al. [47] proposed distinctly different bactericidal mechanisms for Ag nanoparticles and Ag ions. In the silver nitrate treatment, a central region of low molecular weight was formed within the cells as a defense mechanism, whereas no such phenomenon was observed in the nanoparticle treatment, although the nanoparticles did penetrate through the cell wall [48].

In this context, the enhanced bactericidal activity recorded for AgNPs is attributed to their exposure to microorganisms' causes, therefore, irreversible changes in cell wall structure leading to its disruption and affects the integrity of lipid bilayer, the permeability of the cell membrane and the proper regulation of transport activity through the plasma. AgNPs can further penetrate inside the microbial cell and interact with cellular structures and biomolecules such as proteins, lipids, and DNA. The interactions with cellular structures and biomolecules have a damaging effect on microbes. Moreover, silver ions, as a secondary oxidation process of AgNPs, contribute to the biocidal properties of AgNPs by affecting the transport and release of potassium (K^+) ions from the microbial cells [43]. The increase in membrane permeability may lead to more pronounced effects such as loss by leakage of cellular contents, including ions, proteins, reducing sugars and ometimes cellular energy reservoir (ATP) [49].

4. CONCLUSIONS

The present study demonstrates the bio-reductive synthesis of AgNPs within cinnamon extract via microwave irradiation. Cinamonaldehyde-$AgNO_3$ redox couple was successful in reducing silver nitrate to silver nanoparticles. Crystalline spherical shaped Ag nanoparticles were successfully achieved. Water-soluble organics constituting the cinnamon extract were mainly responsible for the Ag ions reduction into nanosized Ag particles. XRD pattern confirmed the face-centered cubic phase of the silver nanocrystals. Media pH played a vital role in Ag nanoparticles development, especially within the alkaline range. Zeta potential values demonstrated the profoundly negative surface charge of the formed nanoparticles and consequent stability. The achieved results demonstrate that the cinnamon extract is biocompatible, cheap and ecofriendly, bio-resource/biomaterial for the Ag nanoparticles synthesis with low cytotoxicity and promising bactericidal activity. The achievement of Ag nanoparticles within cinnamon extract applying the green microwave radiation can be even more attractive if the size of the nanoparticles would be controlled. Conclusively, it is believable to consider nanoparticles as a viable substitute for antibiotics and have a high potential to solve the rise of microbial multidrug-resistance problems.

5. REFERENCES

1. Anupam, R.; Onur, B.; Sudip, S.; Amit, K.M.; Deniz, Y. Green synthesis of silver nanoparticles: biomolecule-nanoparticle organizations targeting antimicrobial activity. *RSC Adv*. **2019**, *9*, 2673-2702, https://doi.org/10.1039/C8RA08982E.
2. Abdel-Fattah, W.; Eid, M.; Abd El-Moez, S.; Mohamed, E.; Ghareib W. Synthesis of biogenic ag@pd core-shell nanoparticles having anti-cancer / anti-microbial functions. *Life Sci.* **2017**, *183*, 28–36, https://doi.org/10.1016/j.lfs.2017.06.017.
3. Arrocha-Arcos, A.A.; Cervantes-Alcalá, R.G.A.; Huerta-Miranda, M.; Miranda-Hernandez, H. Electrochemical reduction of bicarbonate to formate with silver nanoparticles and silver nanoclusters supported on multiwalled carbon nanotubes. *Electro chimica Acta*. **2017**, *246*, 1082-1087, https://doi.org/10.1016/j.electacta.2017.06.147.
4. Shvalagin, V.V.; Grodzyuk, G.Y.; Shvets, A.; Granchak, M.; Lavorik, S.R.; Skorik, N.A. Photochemical reduction of silver and tetrachloroaurate ions on the surface of nanostructured SN_3O_4 under the influence of visible light. *Theor. Exp. Chem.*, **2015**, *51*, 177–182, https://doi.org/10.1007/s11237-015-9413-y.
5. Valverde-Alva, M.A.; García-Fernández, T.; Villagrán-Muniz, M.; Sánchez-Aké, C.; Castañeda-Guzmán, R.; Esparza-Alegría, E.; Sánchez-Valdése C.F.; Sánchez Llamazarese, J., L.; Márquez Herreraf C.E.; Synthesis of silver nanoparticles by laser ablation in ethanol: A pulsed photoacoustic study. *Appl. Surf. Sci.* **2015**, *355*, 341-349, https://doi.org/10.1016/j.apsusc.2015.07.133.
6. Rupak, T.; Chintan, B.; Pragya S.; Suvash, A.; Pravin, D. Enzyme-mediated formulation of stable elliptical silver nanoparticles tested against clinical pathogens and MDR bacteria and development of antimicrobial surgical thread. *Ann. Clin. Microbiol. Antimicrob.* **2017,** *16*, 39, https://doi.org/10.1186/s12941-017-0216-y.
7. Khwaja, S.; Azamal H.; Rifaqat A.K. A review on biosynthesis of silver nanoparticles and their biocidal properties. *Nanobiotechnology*, **2018,** *16*, 14, https://doi.org/10.1186/s12951-018-0334-5.
8. Vijay, K.P.P.N.; Pammi, S.V.N.; Kollu, P.; Satyanarayana, K.V.V.; Shameem U. Green synthesis and characterization of

silver nanoparticles using boerhaavia diffusa plant extract and their antibacterial activity. *Ind. Crops Prod.* **2014**, *52*, 562–566, https://doi.org/10.1016/j.indcrop.2013.10.050.

9. Rathi, S.P.R.; Reka, M.; Poovazhagi, R.; Arul, Kumar, M.; Murugesan, K. Antibacterial and cytotoxic effect of biologically synthesized silver nanoparticles using aqueous root extract of Erythrina indica, Spectrochim. *Acta A Mol. Biomol. Spectrosc.* **2015**, *135*, 1137-44, https://doi.org/10.1016/j.saa.2014.08.019.

10. Malachová K.; Praus P.; Rybková Z.; Kozák O. Antibacterial and antifungal activities of silver, copper and zinc montmorillonites. *Appl. Clay. Sci.* **2011**, *53*, 642–645, https://doi.org/10.1016/j.clay.2011.05.016.

11. Mohammed, F.A.; Girilal, Z.;. Ao, M.; Chen, L.; Xiao, X.; Kalaichelvan, P.; Yao, X. Inactivation of microbial infectiousness by silver nanoparticles-coated condom: a new approach to inhibit HIV- and HSV-transmitted infection. *Int J. Nanomed.* **2012**, *7*, 5007-5018, https://doi.org/10.2147/IJN.S34973.

12. Adhikari, U.; Ghosh, A.; Chandra, G. Nano particles of herbal origin: a recent eco-friend trend in mosquito control. *Asian Pac. J. Trop. Dis.* **2013**, *3*, 167–168, https://doi.org/10.1016/S2222-1808(13)60065-1.

13. Bindhu, M.R.; Umadevi, M. Antibacterial and catalytic activities of green synthesized silver nanoparticles. *Spectrochim. Acta A Mol. Biomol. Spectrosc.* **2015**, *135*, 373-378, https://doi.org/10.1016/j.saa.2014.07.045.

14. Pirtarighat, S.; Ghannadnia, M.; Baghshahi, S.; Green synthesis of silver nanoparticles using the plant extract of *Salvia spinosa* grown in vitro and their antibacterial activity assessment. *J Nanostruct. Chem.* **2019**, *9*, 1-9, https://doi.org/10.1007/s40097-018-0291-4.

15. Mamta, D.; Shikha, D.;Vaishali, S.; Nidhi, R.; Ravi, K. B.; Arvind, K. B.; natural source for the synthesis of silver nanoparticles, *J. Trad. Complement. Med.* **2019**, in press, https://doi.org/10.1016/j.jtcme.2019.04.007.

16. Franco-Romano, M.; Gila, M.L.A.; Palacios-Santanderb, J.M.; Delgado-Jaénc, I.; Naranjo-Rodríguezb, J.J.; Hidalgo-Hidalgo de Cisneros, J.L.; Cubillana-Aguilera, L.M. Sonosynthesis of gold nanoparticles from a geranium leaf extract. *Ultrasonics Sonochem.* **2014**, *21*, 1570-1577, https://doi.org/10.1016/j.ultsonch.2014.01.017.

17. Patcharaporn, T.; Nutthakritta, P.; Parichart, B.; Apiwat, C. Green synthesis of silver nanoparticles in aloe vera plant extract prepared by a hydrothermal method and their synergistic antibacterial activity, *Peer J.* **2016**, *4*, e2589, https://doi.org/10.7717/peerj.2589.

18. Shalaka, A.; Pratik, R.; Vrishali, B.; Suresh, P. Rapid Biosynthesis of Silver Nanoparticles Using Cymbopogan Citratus (Lemongrass) and its Antimicrobial Activity. *Nano-Micro Lett.* **2011**, *3*, 189-194, https://doi.org/10.3786/nml.v3i3.p189-194.

19. Ghareib, W.A.; El-Hotaby, W.; Hemdan, B.; Abdel- Fattah, W.I. Thermosensitive chitosan/phosphate hydrogel-composites fortified with Ag versus Ag@Pd for biomedical applications. *Life Sci.* **2018**, *194*, 185-195, https://doi.org/10.1016/j.lfs.2017.12.021.

20. Chanda, N.; Shukla, R.; Zambre, A.; Mekapothula, S.; Kulkarni, R.; Katti, K.; Bhattacharyya, K.; Fent, M.; Casteel, W.; Boote, J.; Viator, A.; Upendran, A.; Kannan, R.; Katti, V. An effective strategy for the synthesis of biocompatible gold nanoparticles using cinnamon phytochemicals for phantom CT imaging and photoacoustic detection of cancerous cells. *Pharm Res.* **2011**, *28*, 279–291, https://doi.org/10.1007/s11095-010-0276-6.

21. Gow, R.T.; Li, D.; Sypert, G.W.; Alberte, R.S. Extracts and methods comprising cinnamon species. **2007** *US Patent Application Publication US* 2007/0292540 Al.

22. Mathew, S.; Abraham, T.E. Studies on the antioxidant activities of cinnamon (Cinnamomum verum) bark extracts, through various in vitro models. *Food Chem.* **2006**, *94*, 520–528, https://doi.org/10.1016/j.foodchem.2004.11.043.

23. Lopez, P.; Sanchez C.; Batlle R.; Nerin C. Vapor-phase activities of cinnamon, thyme, and oregano essential oils and key constituents against foodborne microorganisms. *J. Agric. Food. Chem.* **2007**, *55*, 4348–4356, https://doi.org/10.1021/jf063295u.

24. Jayaprakasha, K.; Rao, L.J.; Sakariah, K.;K. Chemical composition of volatile oil from Cinnamomum zeylanicum, Z. *Naturforsch.* **2002**, *55*, 990–993, https://doi.org/10.1515/znc-2002-11-1206.

25. Shan, S.; Cai, Y.Z.; Brooks, J.D.; Corke, H. Antibacterial properties and major bioactive components of cinnamon stick (Cinnamomum burmannii): activity against food-borne pathogenic bacteria. *J. Agric. Food Chem.* **2007**, *55*, 5484–5490, https://doi.org/10.1021/jf070424d.

26. Schoene, N.W.; Kelly, M.A.; Polansky, M.M.; Anderson, R.A. Water soluble polymeric polyphenols from cinnamon inhibit proliferation and alter cell cycle distribution patterns of hematologic tumor cell lines. *Cancer Lett.* **2005**, *230*, 134–140, https://doi.org/10.1016/j.canlet.2004.12.039.

27. Aivazoglou, E.; Metaxa, E.; Hristoforou, E. Microwave-assisted synthesis of iron oxide nanoparticles in biocompatible organic environment. *AIP Adv.* **2018,** *8*, 048201, https://doi.org/10.1063/1.4994057.

28. Sgouras, D.; Maragkoudakis, P.; Petraki, K.; Martinez-Gonzalez, B.; Eriotou, E.; Michopoulos, S.; Kalantzopoulos, G.; Tsakalidou, E.; Mentis, A. In vitro and in vivo inhibition of Helicobacter pylori by Lactobacillus casei strain Shirota. *Appl. Environ. Microbiol.* **2004**, *70*, 518-526, https://doi.org/10.1128/aem.70.1.518-526.2004.

29. Abdel-Fattah, W.; Sallam, A.; Attawa, N.; Salama, E.; Maghraby, A.; Ghareib, W. Functionality, antibacterial efficiency and biocompatibility of nanosilver/chitosan/silk/ phosphate scaffolds 1. Synthesis and optimization of nanosilver/chitosan matrices through gamma rays irradiation and their antibacterial activity. *J. Mater., Res. Exp.* **2014**, *1*.

30. Babu, S.M.; Aishwarya, D.; Vidya, S.K.; Saidutta, M.B. Synthesis of silver nanoparticles using medicinal Zizyphus xylopyrus bark extract. *Appl. Nanosci.* **2015**, *5*, 755–762, https://doi.org/10.1007/s13204-014-0372-8.

31. Chen, M.; Chan, C.; Huang, S.; Lin, Y. Green biosynthesis of gold nanoparticles using Chenopodium formosanum shell extract and analysis of the particles' antibacterial properties. *J Sci Food Agric.* **2019**, *99*, 3693-3702, https://doi.org/doi:10.1002/jsfa.9600.

32. Sathishkumar, M.; Sneha, K.; Won, S.W.; Cho, C. W.; Kim, S.; Yun, Y.S. Cinnamon zeylanicum bark extract and powder mediated green synthesis of nano-crystalline silver particles and its bactericidal activity. *Coll. Surf. B Biointerfaces*. **2009**, *73*, 332–338, https://doi.org/10.1016/j.colsurfb.2009.06.005.

33. Sanghi, R.P. Biomimetic synthesis and characterisation of protein capped silver nanoparticles. *Bioresour. Technol.* **2009**, *100*, 501–504, https://doi.org/10.1016/j.biortech.2008.05.048.

34. Manivasagan, P.; Venkatesan, J.; Senthilkumar, K.; Sivakumar, K.; Kim, S.K. Biosynthesis, antimicrobial and cytotoxic effect of silver nanoparticles using a novel Nocardiopsis sp. MBRC-1. *Bio. Med. Res. Int.* **2013,** *1–9*, http://dx.doi.org/10.1155/2013/287638.

35. Karthik, L.; Kumar, G.; Kirthi, A.V.; Rahuman, A.A.; Rao, KVB. Streptomyces sp. LK3 mediated synthesis of silver nanoparticles and its biomedical application. *Bioproc. Biosyst. Eng.* **2013**, *37*, 261–267, https://doi.org/10.1007/s00449-013-0994-3.

36. Annamalai, J.; Nallamuthu, T. Green synthesis of silver nanoparticles: characterization and determination of antibacterial potency. *Appl. Nanosci.* **2016**, *6*, 259–265, https://doi.org/10.1007/s13204-015-0426-6.
37. Deepa, S.: Kanimozhi, K.; Nneerselvam, A. Antimicrobial activity of extra-cellularly synthesized silver nanoparticles from marine derived actinomycetes. *Int. J. Curr. Microbiol. Appl. Sci.* **2013**, 2, 223–230, https://doi.org/10.1016/j.ejar.2016.05.004.
38. Rai, M.; Ingle, A.; Gade, A.; Duarte, M.C.T.; Duran, N. Synthesis of silver nanoparticles by Phoma gardeniae and in vitro evaluation of their efficacy against human disease-causing bacteria and fungi. *IET Nanobiotechnol.* **2015**, *9*, 71–75, https://doi.org/10.1049/iet-nbt.2014.0013.
39. Siriwardana, K.; Wang, A.; Gadogbe, M.; Collier, W.E.; Fitzkee, N.C.; Zhang, D. Studying the Effects of Cysteine Residues on Protein Interactions with Silver Nanoparticles. *J. Phys. Chem. C Nanomater. Interfaces.* **2015,** *119*, 2910–2916, https://doi.org/10.1021/jp512440z.
40. Abdel-Fattah, W.; Nagwa, A.; Ghareib, W. Influence of the protocol of fibroin extraction on the antibiotic activities of the constructed composites. *J. Prog. Biomater.* **2015**, *4*, 77–88, https://doi.org/0.1007/s40204-015-0039-x.
41. Wafa, I.; Abdel Sattar, M.; Diab, A.; Ghareib, W.; Tailoring the properties and functions of phosphate/silk/Ag/chitosan scaffolds. *J. Mater. Sci. Eng. C.* **2015**, *54*, 158–168, https://doi.org/10.1016/j.msec.2015.05.015.
42. Weijia, L.I.; Zhou, J.; Xu, Y. Study of the in vitro cytotoxicity testing of medical devices. *Biomed. Rep.* **2015**, *3*, 617–620, https://doi.org/10.3892/br.2015.481.
43. Dakal, T.C.; Kumar, A.; Majumdar, R.S.; Yadav, V. Mechanistic Basis of Antimicrobial Actions of Silver Nanoparticles. *Front Microbiol.* **2016**, *7* 1831, https://doi.org/10.3389/fmicb.2016.01831.
44. Chung, I.; Park, I.; Seung-Hyun, K.; Thiruvengadam, M.; Rajakumar, G. Plant-mediated synthesis of silver nanoparticles: their characteristic properties and therapeutic applications. *Nanoscale Res. Lett.* **2016**, *11*, 40, https://doi.org/ doi: 10.1186/s11671-016-1257-4.
45. Caroling, G.; Vinodhini, E.; Mercy, A.; Shanthi, P. Biosynthesis of copper nanoparticles using aqueous phyllanthus embilica (gooseberry) extract- characterisation and study of antimicrobial effects. *Int. J. Nano. Chem.* **2015**, *1*, 53-63.
46. Cho, S.H.; Jones, B.L.; Krishnan, S. The dosimetric feasibility of gold nanoparticle-aided radiation therapy (GNRT) via brachytherapy using low-energy gamma-/X-ray sources. *Phys. Med. Biol.* **2009**, *54*, 4889–4905..
47. Xuan, H.; Thi, T.; Thi, T.; Dinh, K.; Xuan, H.; Van-Son, D.; Synthesis and study of silver nanoparticles for antibacterial activity against Escherichia coli and Staphylococcus aureus. *Adv. Nat. Sci: Nanosci. Nanotechnol.* **2018**, *9*, https://doi.org/10.1088/2043-6254/aac58f.
48. Panariti, A.; Miserocchi, G.; Rivolta, I.; The effect of nanoparticle uptake on cellular behavior: disrupting or enabling functions? *Nanotechnol. Sci. Appl.* **2012**, *5*, 87–100, https://doi.org/10.2147/NSA.S25515.
49. Wypij, M.; Czarnecka, J.; Świecimska, M.; Dahm, H.; Rai, M.; Golinska, P. Synthesis, characterization and evaluation of antimicrobial and cytotoxic activities of biogenic silver nanoparticles synthesized from Streptomyces xinghaiensis OF1 strain. *World J. Microbial. Biotechnol.* **2018**, *34*, 23, https://doi.org/10.1007/s11274-017-2406-3.

6. ACKNOWLEDGEMENTS

The authors of the present work are indebted for the financial support presented by the National Research Centre, Giza, Egypt.